Supporting Information

3-D binder-free graphene foam as cathode for high capacity Li-O_2 batteries

Chenjuan Liu,[a] Reza Younesi,[a] Cheuk-Wai Tai,[b] Mario Valvo,[a] Kristina Edström,[a] Torbjörn Gustafsson[a], and Jiefang Zhu[a]*

[a] Department of Chemistry-The Ångström Laboratory, Uppsala University, Box 538, SE-751 21 Uppsala, Sweden.

E-mail: jiefang.zhu@kemi.uu.se; Fax: +46 18 51 3548; Tel: +46 18 471 3722

[b] Department of Materials and Environmental Chemistry, Stockholm University, SE 106 91 Stockholm, Sweden

Table S1: Preparation details for recently reported graphene cathode materials.

Sample	Technology	electrolyte	Free-standing	Ref.
GNSs	1050℃ thermal reduction 30s	1 M $LiPF_6$ in PC/EC (1:1)	No	1
Functionalized graphene sheets	1050℃ thermal reduction 30s	1 M LiTFSI in TEGDME	No (25%PTFE)	2
Nitrogen-doped graphene sheets	900℃ reduced by ammonia	1 M $LiPF_6$ in TEGDME	No (10%PTFE)	3
metal-free GNSs	950℃ reduced by 4%H_2/Ar	1 M $LiClO_4$ in ED/DEC (organic) and 1 M $LiNO_3$ + 0.5 M LiOH (aqueous)	No (7%PTFE)	4
GNSs	Reduced by hydrazine hydrate	1 M $LiClO_4$ in PC	No (10%PTFE)	5
Co-N-MWNTs	Graphitized heteroatom polymer, PANI, high-temperature	1 M $LiPF_6$ in TEGDME	No (9%PVDF)	6
S-GNSs	1050℃ thermal reduction 1h	1 M $LiPF_6$ in TEGDME	No (10%PVDF)	7
N-doped exfoliated graphene	1050℃ thermal reduction 30S	1 M $LiPF_6$ in TEGDME	No (71%PVDF-HFP)	8
Graphene flakes	high-temperature treatment	1 M LiTFSI in DME	No (15%PVDF)	9
Graphene carbon/Ni foam	800℃ thermal treatment 2h in N_2	1 M LiTFSI in DME	Yes	10
Graphene foams	Electrochemical exfoliation	1 M $LiCF_3SO_3$ in TEGDME	Yes	11
GF@Al foam	**300℃ low-temperature treatment**	**1 M $LiClO_4$ in DMSO**	**Yes**	**Our work**

Table S2: Battery properties for recently reported graphene cathode materials.

Sample	Dominant discharge product	Morphology of discharge product	Capacity (mAh/g)	Rechargeability	Ref.
GNSs	Li_2CO_3 (XRD)	film	8705.9 mAh/g at 75 mA/g	unknown	1
Functionalized graphene sheets	Li_2O_2 (XRD)	Particles	15000 mAh/g at ~ 48 mA/g*	unknown	2
N-doped graphene sheets	Li_2O_2 (XRD)	200~500 nm particles	11660 mAh/g at 75 mA/g	unknown	3
metal-free GNSs	unknown	unknown	unknown	50th, (80mAh/g), at 0.5mA/cm^2	4
GNSs	Li_2CO_3 (XRD)	unknown	unknown	5th, at 50mA/g	5
Co-N-MWNTs	Li_2O_2 (XRD)	unknown	3700 mAh/g at 50 mA/g	50th, (1500-1000mAh/g), at 400mA/g	6
S-GNSs	Li_2O_2 (XRD)	Nanorods, nanosheets and toroids in different current	4300 mAh/g at 75 mA/g	unknown	7
N-doped exfoliated graphene	Li_2O_2 (XRD)	unknown	11 746 mAh/g at 70 mA/g	unknown	8
Graphene flakes	Li_2CO_3 (XRD, FT-IR), Li_2O_2 and Li_2O (FT-IR)	Particles	3914 mAh/g at 330 mA/g	unknown	9
Graphene carbon/Ni foam	Li_2O_2 (XRD)	toroidal	11 060 mAh/g at 280 mA/g	10th, (2000mAh/g), at 0.5mA/cm^2	10
Graphene foams	unknown	unknown	unknown	20th, (1000mAh/g), at 100mA/g	11
GF@Al foam	**Li_2O_2, LiOH (XRD)**	**toroidal, spherical, disc shape, and nanosheet-like**	**~ 90000 mAh/g at 100 mA/g**	**27th, (1000mAh/g), at 100mA/g**	**Our work**

**calculated from data reported in the reference.*

It should, however, be noted that different types of binder have been used in most of these graphene-catalyzed cathode materials. It has been shown that binders are unstable in Li-O_2 cells and increase the electrolyte decomposition during cycling, decrease the electrode porosity and the electrical conductivity, while lowering the O_2-diffusion rate[12, 13]. As shown in Table 1, high

temperatures are also often required in the post synthesis treatment processes. Economical factors or technical problems associated with up-scaled production of graphene-catalyzed cathode unfortunately can't be widely addressed. The possibility of utilizing the graphene foam for the design of facile, inexpensive and binder-free electrode described in the present work, is certainly appealing. We therefore feel that our work provides new insight to the oxygen electrode design and that the results presented here may also open up new routes for the fabrication of low-cost and binder-free electrodes for Li-O_2 cells. The tables were added to the supporting information.

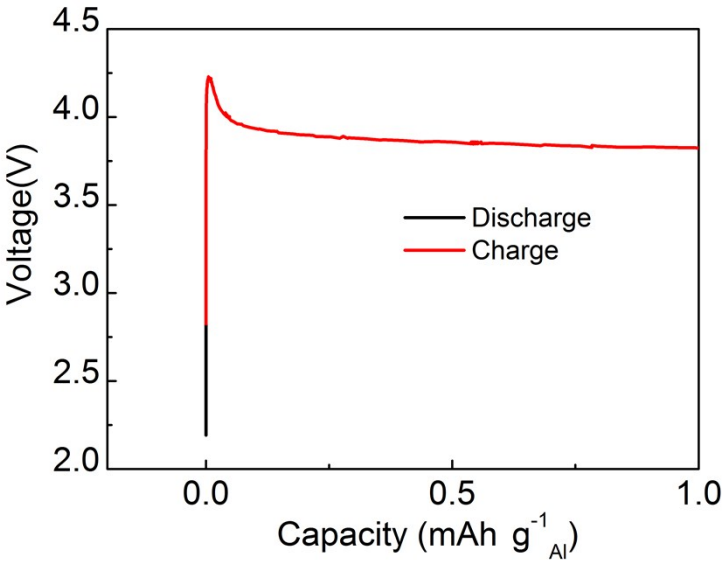

Fig. S1. Discharge-charge curves of Al foam in a Li-O_2 cell using 1 M $LiClO_4$ in DMSO as electrolyte.

The discharge capacity is almost zero. It is the evidence that the Al foam has no contribution in the discharge capacity. Therefore, the charge plateau around 3.9 V represents the oxidation of the electrolyte.

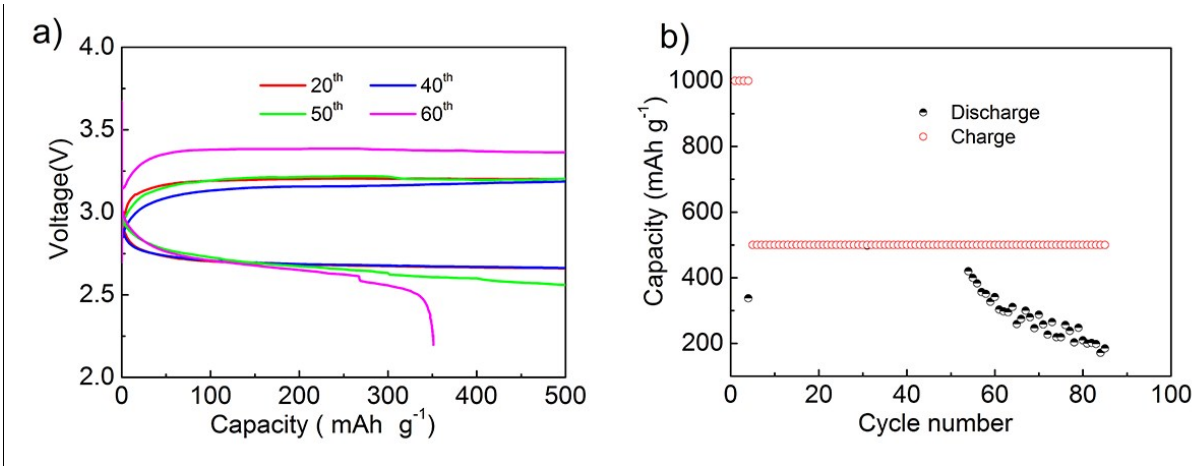

Fig. S2. (a) Charge-discharge curves and (b) cycling performance of GF@Al at a current density of 200 mA g^{-1} with capacity limitation of 1000 mAh g^{-1} for the first 5 cycles and then at current density of 100mA g^{-1} with capacity limitation of 500 mAh g^{-1}.

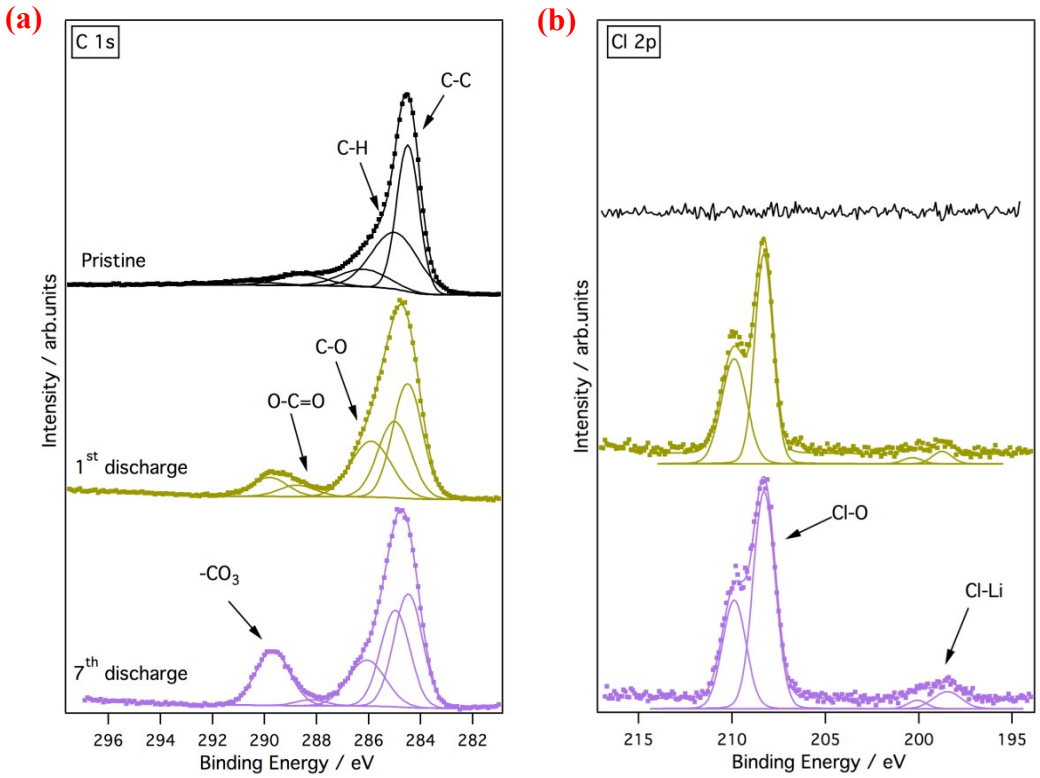

Fig. S3 (a) C 1s and (b) Cl 2p core level XPS spectra of pristine and cycled electrodes after the 1st and the 7th discharge. The discharge capacity was limited to 1000 mAh/g at a current density of 100 mA/g.

The C 1s XPS spectra in Fig. S3 show that some decomposition products containing ether and carboxylate bonds formed on the surface of graphene electrode after the 1st discharge. The results also revealed a noticeable contribution from carbonate ($-CO_3$) decomposition product to the C1s spectrum of the graphene electrode after the 7th discharge. This feature can be correlated with the fact that the Li_2CO_3

side products have been formed after cycling. The 1st and 7th discharge samples contain one main peak at the binding energy of about 208 eV with the spin-orbit split doublets (Cl $2p_{1/2}$) at 1.6 eV higher binding energy ascribed to $LiClO_4$ salt. The other component with lower intensity at about 198.5 eV could be assigned to Cl bonded to elements with low electronegativity (e.g. LiCl).[14] A comparison of the spectra after the 1st discharge and after the 7th discharge shows a moderate increase of the Cl-Li feature, thereby suggesting that additional surface degradation species could have been formed by $LiClO_4$ salt decomposition.

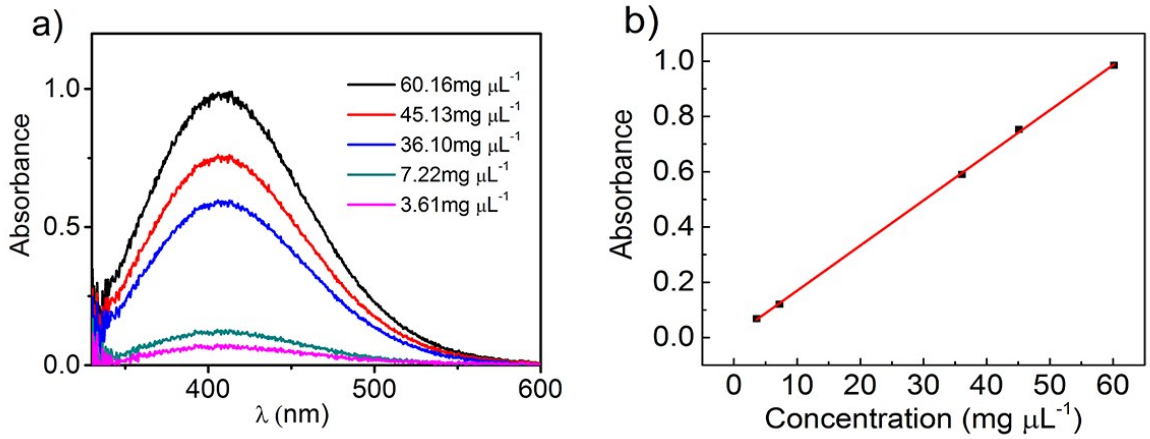

Fig. S4. a) The absorption spectra of $[Ti(O_2^{2-})]^{2+}$ complex originating from the reaction between the Ti(IV)OSO_4 solution and commercial Li_2O_2 of different concentrations. b) The standard absorption curve of $[Ti(O_2^{2-})]^{2+}$ complex derived from a).

Before the analysis of our cathodes, commercial Li_2O_2 was used to establish a standard titration curve. A given amount of Li_2O_2 was dissolved into an aqueous solution of Ti(IV)OSO_4. The Li_2O_2 reacted with H_2O and produced H_2O_2 .The subsequent reaction between H_2O_2 and Ti(IV)OSO_4 forms a yellow $[Ti(O_2^{2-})]^{2+}$ complex with a broad absorption peak at 405 nm,[15] as shown in the following reaction schemes:

$$Li_2O_2 + 2H_2O \rightarrow 2LiOH + H_2O_2$$

$$Ti(IV)OSO_4 \rightarrow [Ti(O_2^{2-})]^{2+}$$

By dissolving different amounts of Li_2O_2 into the Ti(IV)OSO_4 aqueous solution we observed a linear relationship between the concentration of Li_2O_2 and the characteristic extinction of the

$[Ti(O_2^{2-})]^{2+}$ as shown in Fig. S3. This allows for a quantification of the amount of Li_2O_2. The discharged cathodes were immersed in an aqueous solution of $Ti(IV)OSO_4$ to quantify the discharge product Li_2O_2 based on the standard titration curve.

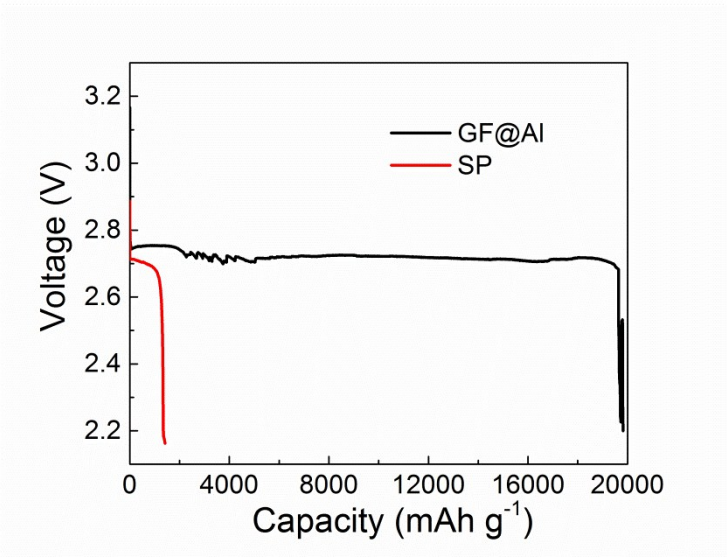

Fig. S5 the discharge curve of SP and GF@Al cathode for titriation

Table S3. Discharge Li_2O_2 percent yields (Y_{Li2O2}) for different cathode materials

electrolyte	cathode	Capacity(mAh g^{-1})	Y_{Li2O2} (%)
1M $LiClO_4$/DMSO	GF@Al	2×10^4	33.7±4.4
1M $LiClO_4$/DMSO	SP	1.4×10^3	49.3±4.9

The data in Table S3 were acquired from GF@Al and SP electrodes at the current density of 100 mA g^{-1}. The Y_{Li2O2} values are calculated by using the following equation:

$$Y_{Li2O2} = {}^{m_{Li_2O_2,t}}\Big/_{m_{Li_2O_2,e}}$$

where $^{m_{Li_2O_2,t}}$ and $^{m_{Li_2O_2,e}}$ are the amount of Li_2O_2 by titration and the calculated amount by expected given a 2 e^-/ Li_2O_2 process during discharge (0.857 mg Li_2O_2 per mAh would be expected given a 2 e^-/ Li_2O_2 process), respectively.

The surface density and thickness of Li_2O_2 on ideal single layer graphene surface after full discharge were calculated from the formula as follows:

$$\bar{m} = \frac{m_{Li_2O_{2,}e}}{a_{GF}} = \frac{Q \times 0.857\ mg\ mAh^{-1}}{A_{GF}} = \frac{9 \times 10^4 mAh \cdot g^{-1} \times 0.857\ mg\ mAh^{-1}}{2630 m^2\ g^{-1}} \approx 3 \times 10^{-3} mg\ cm^{-2}$$

$$d_{Li_2O_{2,}e} = \frac{\bar{m}}{\rho_{Li_2O_{2,}}} = \frac{3 \times 10^{-3} mg\ cm^{-2}}{2.31 \times 10^3 mg\ cm^{-3}} \approx 13nm$$

In which $m_{Li_2O_{2,}e}$ is the calculated mass of Li_2O_2 with the given 2 e^-/ Li_2O_2 process during discharge, Q is the discharge capacity, $\bar{m}$ is the mass of the Li_2O_2 product on average graphene surface, a_{GF} and A_{GF} are the theoretical surface area and specific surface area of graphene, and $d_{Li_2O_{2,}e}$ is the thickness of calculated Li_2O_2 on graphene surface.

When the layer of graphene n is not a single layer:

n=2, $d_{Li_2O_{2,}e} = 26\ nm$

n=3, $d_{Li_2O_{2,}e} = 39\ nm$

n=4, $d_{Li_2O_{2,}e} = 52\ nm$

Even with a multilayer structure graphene, the calculated Li_2O_2 thickness is still at a reasonable range.

References

1. Y. Li, J. Wang, X. Li, D. Geng, R. Li and X. Sun, *Chem Commun (Camb)*, 2011, **47**, 9438-9440.
2. J. Xiao, D. H. Mei, X. L. Li, W. Xu, D. Y. Wang, G. L. Graff, W. D. Bennett, Z. M. Nie, L. V. Saraf, I. A. Aksay, J. Liu and J. G. Zhang, *Nano Lett*, 2011, **11**, 5071-5078.
3. Y. L. Li, J. J. Wang, X. F. Li, D. S. Geng, M. N. Banis, R. Y. Li and X. L. Sun, *Electrochem Commun*, 2012, **18**, 12-15.
4. E. Yoo and H. Zhou, *Acs Nano*, 2011, **5**, 7.
5. B. Sun, B. Wang, D. Su, L. Xiao, H. Ahn and G. Wang, *Carbon*, 2012, **50**, 727-733.
6. G. Wu, N. H. Mack, W. Gao, S. G. Ma, R. Q. Zhong, J. T. Han, J. K. Baldwin and P. Zelenay, *Acs Nano*, 2012, **6**, 9764-9776.
7. Y. Li, J. Wang, X. Li, D. Geng, M. N. Banis, Y. Tang, D. Wang, R. Li, T.-K. Sham and X. Sun, *J Mater Chem*, 2012, **22**, 20170.

8. D. Higgins, Z. Chen, D. U. Lee and Z. Chen, *J Mater Chem A*, 2013, **1**, 2639.
9. S. Y. Kim, H. T. Lee and K. B. Kim, *Phys Chem Chem Phys*, 2013, **15**, 20262-20271.
10. Z.-L. Wang, D. Xu, J.-J. Xu, L.-L. Zhang and X.-B. Zhang, *Adv Funct Mater*, 2012, **22**, 3699-3705.
11. W. Zhang, J. Zhu, H. Ang, Y. Zeng, N. Xiao, Y. Gao, W. Liu, H. H. Hng and Q. Yan, *Nanoscale*, 2013, **5**, 9651-9658.
12. E. Nasybulin, W. Xu, M. H. Engelhard, Z. Nie, X. S. Li and J.-G. Zhang, *J Power Sources*, 2013, **243**, 899-907.
13. C. V. Amanchukwu, J. R. Harding, Y. Shao-Horn and P. T. Hammond, *Chem Mater*, 2015, **27**, 550-561.
14. J. F. Moulder, W. F. Stickle, P. E. Sobol and K. D. Bomben, *Handbook of X-ray Photoelectron Spectroscopy,* Physical Electronics, Eden Prairie, MN (2000).
15. D. W. O'Sullivan and M. Tyree, *International Journal of Chemical Kinetics*, 2007, **39**, 457-461.